Bioresource Technology 148 (2013) 414–421

Contents lists available at ScienceDirect

Bioresource Technology

journal homepage: www.elsevier.com/locate/biortech

The adsorption behavior and mechanism investigation of Pb(II) removal by flocculation using microbial flocculant GA1

Jing Feng, Zhaohui Yang *, Guangming Zeng, Jing Huang, Haiyin Xu, Yuanyuan Zhang, Shumei Wei, Like Wang

College of Environmental Science and Engineering, Hunan University, Changsha 410082, PR China
Key Laboratory of Environmental Biology and Pollution Control, Hunan University, Ministry of Education, Changsha 410082, PR China

HIGHLIGHTS

- MBFGA1 was used in two stages to remove Pb(II) ions from aqueous solution.
- Pb(II) adsorption could be described by the Langmuir adsorption model.
- The adsorption process could be described by pseudo-second-order kinetic model.
- The main mechanisms could be charge neutralization and adsorption bridging.

ARTICLE INFO

Article history:
Received 26 June 2013
Received in revised form 30 August 2013
Accepted 1 September 2013
Available online 11 September 2013

Keywords:
Microbial flocculants
Pb(II)
Adsorption
Mechanism investigation

ABSTRACT

In this work, microbial flocculant GA1 (MBFGA1) was used to remove Pb(II) ions from aqueous solution. A series of experimental parameters including initial pH, MBFGA1 dose, temperature and initial calcium ions concentration on Pb(II) uptake was evaluated. Meanwhile, the flocculation mechanism of MBFGA1 was investigated. The removal efficiency of Pb(II) reached up to 99.85% when MBFGA1 was added in two stages, separately. The results indicated that Pb(II) adsorption could be described by the Langmuir adsorption model, and being the monolayer capacity negatively affected with an increase in temperature. The adsorption process could be described by pseudo-second-order kinetic model. Fourier transform-infrared spectra and environmental scanning electron microscope analysis indicated that MBFGA1 had a large number of functional groups, which had strong capacity for removing Pb(II). The main mechanisms of Pb(II) removal by MBFGA1 could be charge neutralization and adsorption bridging.

1. Introduction

Heavy metals, such as Cr(VI), Cu(II), Pb(II), Zn(II), Cd(II), etc., are discharged into surface water increasingly. They are nondegradable and tend to accumulate along the food chain and many heavy metal ions are known to be toxic or carcinogenic. Pb(II), as one of most toxic heavy metals, exists in the wastewater of many industries, like plating, tanneries, oil refining, and mining (Schneegurt et al., 2001). The presence of Pb(II) in drinking water, even at low concentrations, may cause human diseases like anemia, hepatitis, nephrite syndrome, kidney failure, nervous diseases, etc. (Xu et al., 2008; Karatas, 2012). The control of Pb(II) pollution in wastewater is of great significance.

Nowadays, there are many techniques for the removal of Pb(II) ions from wastewater such as chemical precipitation, ion exchange, adsorption, filtration, electrochemical treatment, coagulation and flocculation (Fu and Wang, 2011). However, these techniques have several disadvantages such as incomplete metal removal, high reagent and energy consumption and a mass of floc residuals with their degraded monomers (e.g., monomers of polyacrylamide derivatives) that require disposal and further treatment (Chakravarty et al., 2010). It is becoming increasingly important to find an effective and eco-friendly method to remove Pb(II) from industrial wastewater.

Microbial flocculants (MBFs), microorganism-produced secondary metabolites through fermentation, extraction, refining, can flocculate suspended solids, cells, colloidal solids, etc. (Salehizadeh and Shojaosadati, 2001).With the advantages of high security, high efficiency, non-toxicity and biodegradability over traditional flocculants, MBFs have increasingly attracted wide attention recently (Zhang et al., 2007). The flocculation mechanisms of MBFs are not entirely clear analyzing by systematically studying in previous works. A series of flocculation mechanisms for MBFs, like adsorption bridging, charge neutralization and precipitation

---

* Corresponding author at: College of Environmental Science and Engineering, Hunan University, Changsha 410082, PR China. Tel./fax: +86 0731 88822829.
E-mail address: yzh@hnu.edu.cn (Z. Yang).

0960-8524/$ - see front matter © 2013 Elsevier Ltd. All rights reserved.
http://dx.doi.org/10.1016/j.biortech.2013.09.011

enmeshment, were proposed. The adsorption bridging mechanism is more often used to explain flocculation mechanism for MBFs. Studying the flocculation mechanism could help us to understand the role of MBFs in wastewater treatment and to improve the actual treating effects.

A number of investigations using different MBFs for the treatment of different types of wastewater have been carried out, such as decolorization for dye solution, improving performance of activated sludge and removing suspended solids (SS) (Lian et al., 2008; Gao et al., 2009). In addition, MBFs belong to a kind of extracellular polymeric substances (EPS) that are complex mixtures of macromolecular polyelectrolytes. They are variable molecular mass and characterized with structural properties including polysaccharides, proteins and nucleic acids (Shih et al., 2001). Depending on the chemical composition and structure, MBFs exhibit ability to bind with metal ions. Therefore, it is interesting to investigate the possible application of MBFs to remove heavy metals, such as Pb(II).

MBFGA1 is a kind of microbial flocculant harvested from the fermentation liquid of *Paenibacillus polymyxa* GA1. In our previous studies, we had optimized its flocculation conditions of removing Cu(II), Cd(II) and residual aluminum (Gao et al., 2011; Huang et al., 2012). It is relatively effective, eco-friendly, simple and inexpensive to operate. The main objective of this research was to investigate the ability of MBFGA1 to remove Pb(II) from aqueous solution and explore the flocculation mechanism based on the experimental results.

2. Methods

2.1. Reagents

$Pb(NO_3)_2$ (Fuchen Chemicals, China) was prepared by dilution of 1 g L^{-1} stock solution. Fresh diluents were used in each experiment. $CaCl_2$ (Sanpu Chemicals, China) was prepared at the concentration of 10 g L^{-1}. NaOH, HCl, EDTA and CH_4N_2O were prepared at the concentration of 0.5 mol L^{-1}. Unless otherwise stated, all reagents used were analytically pure.

2.2. MBFGA1 (bacteria strain and culture conditions)

GA1, flocculant-producing strain CCTCC M206017, which was identified as *P. polymyxa* by 16S rDNA sequence and its biochemical and physiological characteristics, was screened from the soil collected in the Yuelu Mountain, Changsha, China (Yang et al., 2006).

The seed medium was prepared as follows: peptone 10.0 g, beef extract 3.0 g and NaCl 5.0 g were added into 1 L distilled water with the pH adjusted to 7.0. All media solutions were prepared with distilled water. The steam sterilization lasted 30 min at 121 °C. After the inoculation of the seed medium, the GA1 was cultured on the roundabout shaker at 150 rpm and 30 °C for 24 h. The fermentation medium consisted of sucrose 40.0 g, yeast extract 4.0 g, K_2HPO_4 5.0 g, KH_2PO_4 2.0 g, NaCl 0.1 g and $MgSO_4$ 0.2 g dissolved in 1 L distilled water with the pH adjusted to 7.0. The steam sterilization lasted 30 min at 115 °C. And this cultivated process was divided into two stages. In the first 24 h, the medium was incubated at 30 °C and was shaken at 150 rpm which provided a positive effect for the growth of the bacteria. In the following 48 h, the rotating speed of shaker was decelerated to 100 rpm and the temperature was decreased to 25 °C, since this conditions was favorable to the yield of MBFGA1. After 72 h of cultivation, the fermentation liquid with 13.35 g L^{-1} effective components was stored at 4 °C, and it would be utilized directly in the flocculation. The effective components mainly were polysaccharides (Zhang et al., 2013).

2.3. Flocculation and adsorption tests

A standard Jar Tester was used for the flocculation and adsorption tests in aqueous $Pb(NO_3)_2$ solution dosed with MBFGA1. $CaCl_2$ and MBFGA1 were added into 1000 mL of $Pb(NO_3)_2$ solution in 1000 mL beaker in turn and then fixed on the floc-tester (ET-720, Lovibond, Germany). The pH of the mixture was adjusted by NaOH and HCl. Flocculation was the first stage, began with 1 min rapid mixing at 150 rpm and ended with 2 min slow mixing at 40 rpm (Yang et al., 2009). The slow mixing after the first stage was the second stage, about adsorption. The influence of the flocculation parameters, including MBFGA1, $CaCl_2$ and pH, was investigated by analyzing the removal efficiency of Pb(II) and the Zeta potentials of the flocculation systems. The concentrations of Pb(II) were determined by flame atomic absorption spectrometry (Modle AAnalyst 700, Perkin–Elmer, USA) after being filtered by 0.45 μm filter membrane. The removal efficiency (RE) and removal capacity of Pb(II) was calculated as follows:

$$\mathrm{RE}\,(\%) = (C_0 - C_e)/C_0 \times 100 \qquad (1)$$

$$\text{Removal capacity} = (C_0 - C_e)V/w_{GA1} \qquad (2)$$

where C_0 and C_e are the initial and equilibrium concentrations of Pb(II) (mg L^{-1}), respectively. V is the volume of Pb(II) solution (L) and w_{GA1} is the weight of MBFGA1.

The variation of Zeta potential during the process of flocculation was monitored by Zetasizer (Nano-ZS90, Malvern, England). Samples were carried out at different time points: $Pb(NO_3)_2$ solution at pH 8, after adding MBFGA1, after adding $CaCl_2$ and during flocculation process. All experiments were performed in triplicates for the mean calculation.

The investigations on adsorption isotherm and adsorption kinetics were also carried out in order to understand the adsorption behavior of Pb(II) during the flocculation process. Isotherm studies were conducted by contacting $2 \times 10^{-3} + 4 \times 10^{-3}$% (w/w) MBFGA1 ($2 \times 10^{-3}$ and 4×10^{-3}% (w/w) MBFGA1 was added in two stage, separately) into 1000 mL Pb(II) solution at different initial concentration (40, 45, 50, 55 and 60 mg L^{-1}) with the solution stirring for 90 min. The experiments were performed at different temperature (20, 30 and 40 °C) by water bath. Sorption isotherms are plots of the equilibrium adsorption capacity (q_e) (according to Eq. (2)) versus the equilibrium concentration of the residual Pb(II) in the solution (C_e).

And the equilibrium uptake was calculated by Eq. (2):

$$q_e = (C_f - C_e)V/W \qquad (3)$$

$$W = (C_0 - C_f)V + w_{GA1} \qquad (4)$$

where q_e is the equilibrium capacity of Pb(II) on the adsorbent (mg g^{-1}) and C_0 is the initial concentration of Pb(II) (mg L^{-1}). C_f is the concentration of Pb(II) after first stage (mg L^{-1}). C_e is the equilibrium concentration of Pb(II) (mg L^{-1}). V is the volume of Pb(II) solution (L). W is the weight of adsorbent (g) and w_{GA1} is the weight of MBFGA1. All the batch experiments were carried out in triplicate and the values reported here were the averages of three readings.

To investigate the kinetic characteristics of the adsorption, $2 \times 10^{-3} + 4 \times 10^{-3}$% (w/w) MBFGA1 was added to 1000 mL of Pb(II) solution with three different concentration (40, 50 and 60 mg L^{-1}), and the samples were stirred for designated time.

Following the Pb(II) adsorption experiment, Pb(II)-loaded MBFGA1 were separated by filtration and suspended into 20 ml of HCl (0.5 mol L^{-1}), EDTA (0.5 mol L^{-1}) and CH_4N_2O (0.5 mol L^{-1}), respectively.

2.4. Fourier transform-infrared spectra (FT-IR) and environmental scanning electron microscope (ESEM) analysis

Fourier transform-infrared spectrometer (TENSOR27, BRUKER, Germany) was employed to examine the interactions between the Pb(II) ions and MBFGA1. Original samples and flocs which MBFGA1 flocculated Pb(II) under the optimal experimental conditions were collected, followed by vacuum freeze-drying. The samples were ground well to make KBr pellets under hydraulic pressure of 400 kg cm^{-2} and spectra were recorded in the range of 400–4000 cm^{-1}. In each scan, the amounts of the sample and KBr were kept constant in order to know the changes in the intensities of characteristic peaks with respect to the structural changes.

The surface morphology of original and Pb(II)-loaded MBFGA1 were also studied using an environmental scanning electron microscope (ESEM) (Quanta 200 FEG, FEI, USA) in low vacuum mode at an acceleration potential of 20 kV. Furthermore, microanalysis of the Pb(II)-loaded MBFGA1 was carried out with an energy dispersive spectrometer (EDS) equipped on the Quanta 200.

3. Results and discussion

An analysis of experimental results indicated the influence of operating conditions on the flocculation and adsorption process.

3.1. Removal efficiency and adsorption capacity in different experiment conditions

3.1.1. Effect of MBFGA1 dose on the flocculantion behavior

The effect of MBFGA1 dose on the flocculation of Pb(II) was investigated by adding $4 \times 10^{-3}\%$ (w/w) $CaCl_2$ and different mass fraction of MBFGA1 into 1 L $Pb(NO_3)_2$ solution (50 mg L^{-1}) with pH value fixed at 8.0. MBFGA1 was added before rapid mixing (first stage) and after two minutes' slow mixing (second stage). As can be seen from Fig. 1(a), at the first stage, the removal efficiency of Pb(II) increased, and then decreased with increasing addition of MBFGA1. The maximum removal efficiency reached about 73% when $2 \times 10^{-3}\%$ (w/w) MBFGA1 was added. Less dose of MBFGA1 meant less MBFGA1 molecules adsorbed Pb(II), and fewer bridges were developed between them. Further increase of MBFGA1 led to a drastic decrease of the removal efficiency of Pb(II), for the reason that more doses of MBFGA1 would inhibit small flocs to grow into big ones. As a result of stronger repulsion force between flocs, they could be deflocculated. After the first stage, the residential concentration of Pb(II) was still high, so MBFGA1 needed to be added again based on the preliminary tests. At the second stage, the removal efficiency of Pb(II) exceeded 90%. When $4 \times 10^{-3}\%$ (w/w) MBFGA1 was added, it can reach about 99.85%. The removal capacity showed the same tendency to removal efficiency after the second stage. Like other flocculating agents, the dose of MBFGA1 should be optimized because more or less dose would be unfavorable to the flocculation.

3.1.2. Effect of $CaCl_2$ on the flocculantion behavior

The effect of $CaCl_2$ on the flocculating efficiency of MBFGA1 was investigated by adding different volume of $CaCl_2$ and $2 \times 10^{-3} + 4 \times 10^{-3}\%$ (w/w) MBFGA1 into 1 L $Pb(NO_3)_2$ solution (50 mg L^{-1}) with pH value fixed at 8.0. Fig. 1(b) indicated that the removal efficiency of Pb(II) was low without adding $CaCl_2$. With further addition of $CaCl_2$, the removal efficiency of Pb(II) increased. The maximum amount of removal capacity reached 831.5 mg g^{-1} when $4 \times 10^{-3}\%$ (w/w) $CaCl_2$ were added. During the flocculating process, the main role of $CaCl_2$ was to provide Ca^{2+} as a kind of coagulant aid. Ca^{2+} could increase the initial adsorption capacity of MBFGA1 by decreasing the negative charge on both the polymer and the particle. It also reduced the absolute values of Zeta potential in the flocculation system, which was consistent with the results of some researchers (Sobeck and Higgins, 2002; Prasertsan et al., 2006; Li et al., 2008). Ca^{2+} ions have also been reported to develop bridges between anionic polyelectrolytes and negatively-charged colloidal particles, thereby enhancing particle flocculation (Lee et al., 2012).

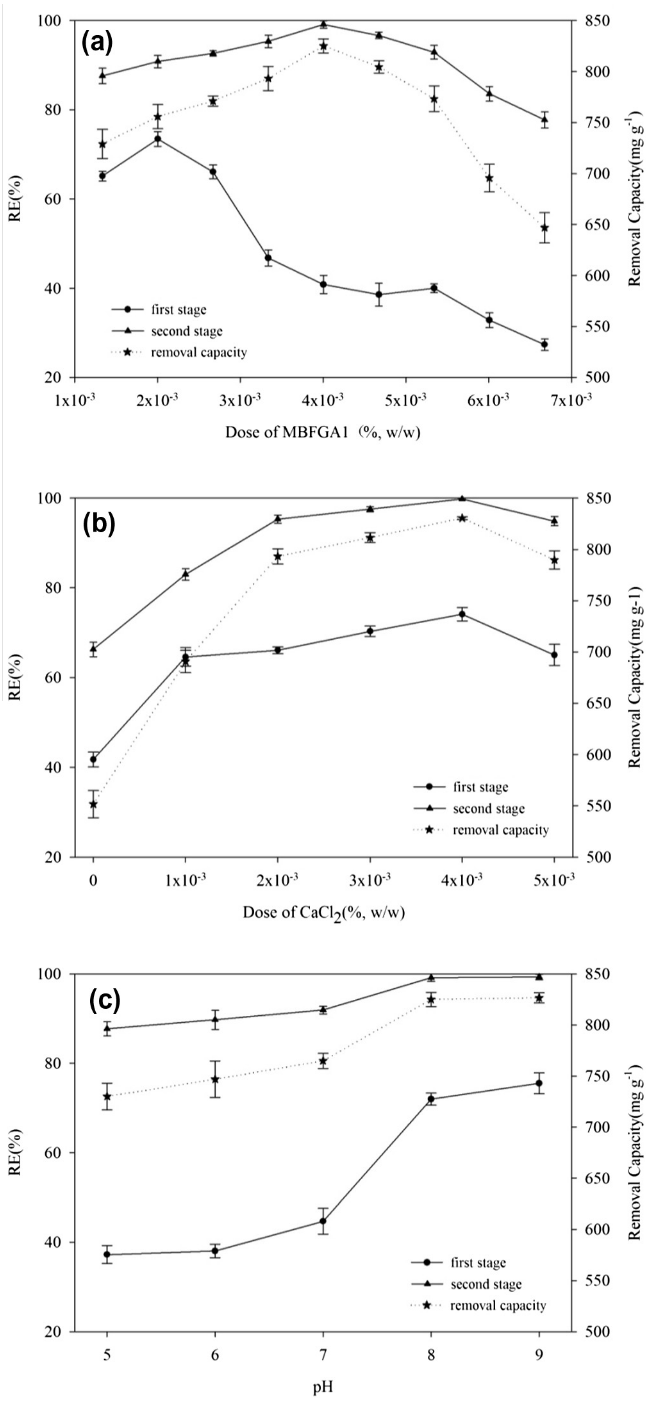

Fig. 1. Effect of (a) MBFGA1 dose, (b) $CaCl_2$ and (c) pH on the flocculation.

3.1.3. Effect of pH on the flocculantion behavior

The effect of pH on the flocculation adsorption of Pb(II) ions onto MBFGA1 was studied by changing initial pH values over the range of 5–9 and adding $4 \times 10^{-3}\%$ (w/w) $CaCl_2$ and

$2 \times 10^{-3} + 4 \times 10^{-3}$% (w/w) MBFGA1 into 1 L $Pb(NO_3)_2$ solution (50 mg L^{-1}). The results were presented in Fig. 1(c). The removal efficiency of Pb(II) improved as initial pH of solution increased, which may be attributed to the existence of hydrogen ions that could strongly compete with Pb(II). At the same time, the activity of functional groups with good flocculation effect of MBFGA1 such as hydroxyl, carboxyl, methoxyl and their competition for flocculation adsorption of metallic ions were affected by pH. The maximum flocculation adsorption for Pb(II) ions was found to be more than 99% at pH 8–9. However, at higher pH values, the flocculation adsorption yield for Pb(II) did not increase any more. While the pH values were lower than 7, the flocculation adsorption yield was in the range of 80–90% for Pb(II). These results could be explained by the pH effect on both metal binding sites on the biomass surface and metal chemistry in aqueous solutions. Increased positive charge (protons) density on the surface of biomass at low pH values restricted the approach of Pb(II) as a result of repulsive force. In contrast, when the pH values increased, adsorbent surfaces were negatively charged and the adsorption of Pb(II) would reach the maximum around pH 8–9. When the pH values exceeded 9, due to the formation of soluble hydroxide complexes of the metal ions and their competition with the active sites, the adsorption of Pb(II) was complicated and cannot be described by simple models. A similar theory was proposed by several researchers studying the adsorption of Pb(II) on different biomasses (Yan and Viraraghavan, 2003; Karthikeyan et al., 2007). Therefore, all the other adsorption experiments were carried out at pH 8.

Table 1 showed the removal capacities of some biosorbents on relevant works previously. The removal capacity of MBFGA1 for Pb(II) was higher than majority of other biomasses that have been mentioned. Therefore, it could be noteworthy that MBFGA1 has important potential for the removal of Pb(II) ions from aqueous solution.

3.2. Adsorption isotherm studies

To identify the efficacy and the mechanism of the adsorption process, Langmuir and Freundlich models were used in this study. The Langmuir adsorption isotherm assumes that adsorption occurs at specific homogeneous sites within the adsorbent and can be represented as:

$$q_e = K_L q_{max} C_e/(1 + K_L C_e) \quad (5)$$

where C_e is the equilibrium concentration of Pb(II) (mg L^{-1}). q_e is the amount of Pb(II) adsorbed (mg g^{-1}). K_L (L g^{-1}) is the equilibrium adsorption constant which is related to the affinity of the binding sites and q_{max} (mg g^{-1}) is the maximum amount of Pb(II) per unit mass of adsorbent when all the binding sites are occupied. The Langmuir parameters can be determined from a linearized form of Eq. (5):

$$C_e/q_e = 1/(K_L q_{max}) + C_e/q_{max} \quad (6)$$

The experimental data were plotted as C_e/q_e versus C_e and shown in Fig. 2(a).

The essential feature of the Langmuir isotherm can be expressed by means of a separation factor or equilibrium parameter R_L, which is calculated by the following equation:

$$R_L = 1/(1 + K_L C_0) \quad (7)$$

where K_L (L mg^{-1}) is the Langmuir constant and C_0 (mg L^{-1}) is the highest initial concentration of Pb(II).The Freundlich equation is given by:

$$q_e = K_f - C_e^{1/n} \quad (8)$$

where K_f (mg g^{-1}) and n are the Freundlich constants and are related to the adsorption capacity of the adsorbent and the adsorption intensity. To simplify the determination of K_F and $1/n$, Eq. (8) can be linearized in logarithmic form which allows the determination of the unknown parameters by plotting log q_e versus log C_e:

$$\log q_e = \log K_f + 1/n \log C_e \quad (9)$$

The experimental data were plotted as log q_e versus log C_e and shown in Fig. 2(b).

The values of Langmuir and Freundlich constants were obtained by linear regression method and the results were shown in Table 2. Within the studied temperature range, the experimental data exhibited higher correlation with Langmuir model than Freundlich model (based on the higher correlation coefficient i.e. R^2 value). From Langmuir model, the q_{max} decreased and K_L increased with temperature rising. This suggested the affinity between the active sites of the MBFGA1 and Pb(II) and also between the adjacent molecules of the adsorbed phase would be stronger at higher temperature in comparison to lower temperature (Ghorai et al., 2012). That all R_L values obtained were between 0 and 1 indicated the adsorption of Pb(II) by MBFGA1 was favorable. This meant that Langmuir model could well describe the equilibrium isotherms, and the adsorption process was monolayer surface adsorption with finite number of identical sites, which were homogeneously distributed on the adsorbent surface (Hu et al., 2011).

3.3. Adsorption kinetic studies

To investigate the mechanism of adsorption and its potential rate-controlling steps that include mass transport and chemical reaction processes, kinetic models have been used to analyze the experimental data. In addition to clarifying the adsorption kinetics of Pb(II) onto MBFGA1, two kinetic models, pseudo-first-order and pseudo-second-order were applied. The linearized form of the pseudo-first-order rate equation was given as:

$$\log(q_e - q_t) = \log q_e - k_1 t/2.303 \quad (10)$$

where q_e and q_t are the amounts of adsorbed Pb(II) on MBFGA1 at equilibrium and at time, respectively (mg g^{-1}), and k_1 is the first-order adsorption rate constant (min^{-1}).

The linearized form of the pseudo-first-order model for the sorption of Pb(II) onto MBFGA1 at various initial concentrations was given in Fig. 3(a). The calculated results of the pseudo-first-order rate equation were given in Table 3. It was found that correlation coefficients values were low, indicating the bad linearization. Additionally, the q_e value acquired by this method was contrasted with the experimental value. So the reaction could not be classified as pseudo-first-order.The pseudo-second-order equation was given as:

Table 1
Biosorbents used for metal removal (mg g^{-1}).

Biosorbents	Removal capacity	References
Saccharomyces cerevisiae	30.04	Çabuk et al. (2007)
Penicillium sp.	72.5	Velmurugan et al. (2010)
Pestalotiopsis sp.	51.9	Moon et al. (2006)
P. chrysosporium	86.9	Kogej and Pavko (2001)
R. nigricans	83.5	Kogej and Pavko (2001)
Turbinaria conoides	439.4	Senthilkumar et al. (2007)
Mimosa pudica inoculated with *Cupriavidus taiwanensis*	485.0	Chen et al. (2008)
Marine algae ER95Ca	263.6	Matheickal and Yu (1999)
MBFGA1	831.5	This study

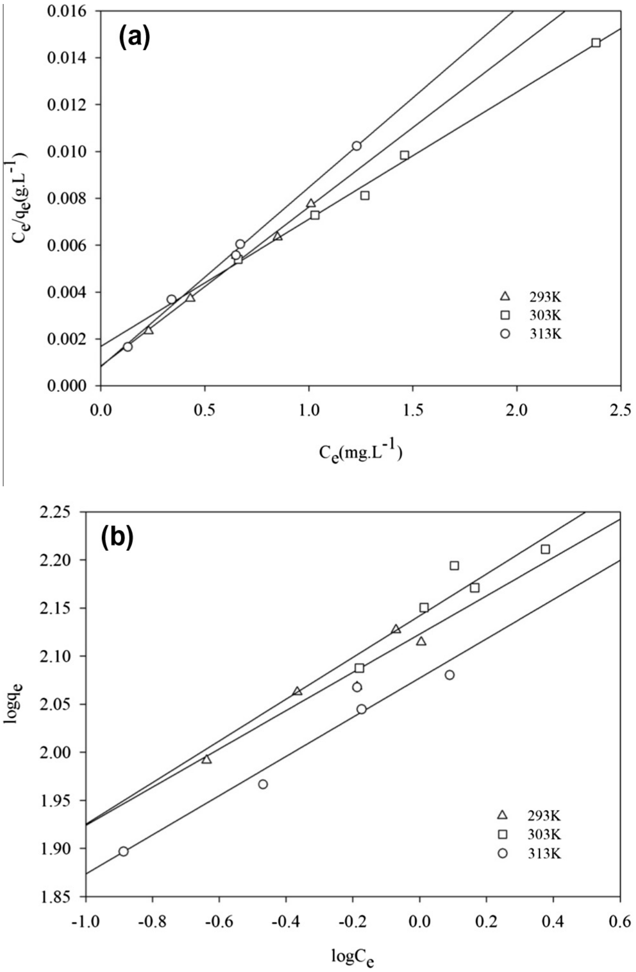

Fig. 2. (a) Langmuir and (b) Freundlich isotherm models for Pb(II) adsorption onto MBFGA1 at different temperatures.

$$t/q_t = 1/(k_2 q_e^2) + 1/(q_e^t) \tag{11}$$

where k_2 is the second-order adsorption rate constant (g mg^{-1} min^{-1}), and q_e is the adsorption capacity calculated by the pseudo-second-order kinetic model (mg g^{-1}).

The linearized form of the pseudo-second-order model for the sorption of Pb(II) onto MBFGA1 at various initial concentrations was given in Fig. 3(b). The values of the correlation coefficients were extremely high and all greater than 0.999. Besides, the calculated q_e values matched very well with the experimental data. These results suggested that the adsorption of Pb(II) onto MBFGA1 followed well the pseudo-second-order kinetic model. Thus experiment results supported the assumption that the rate limiting step in adsorption of heavy metals are chemisorption involving valence forces through the sharing or exchange of electrons between adsorbent and metal ions (Aydın and Aksoy, 2009).

3.4. Thermodynamics parameters

The effect of temperature on the adsorption of Pb(II) onto MBFGA1 was given from the calculated thermodynamic parameters (Table 6). The thermodynamic parameters ($\Delta G°$, $\Delta H°$, $\Delta S°$) were calculated from following equations:

$$\Delta G^{\circ} = -RT \ln K_D \tag{12}$$

$$\Delta G^{\circ} = \Delta H^{\circ} - T\Delta S^{\circ} \tag{13}$$

$$\ln K_D = \Delta S^{\circ}/R - \Delta H^{\circ}/RT \tag{14}$$

where R is the universal gas constant (8.314 J mol^{-1} K^{-1}) and T is the temperature (K). K_D is the distribution coefficient equal to q_e/C_e (L g^{-1}) (Sarı et al., 2007). The Gibbs free energy change of the process was related to the distribution coefficient (K_D) in the linearized form of Eq. (13).

The values of $\Delta G°$ were negative at all temperatures, confirming that the adsorption of Pb(II) onto MBFGA1 was spontaneous and thermodynamically favorable. The increase in $\Delta G°$ values with increase temperature showed an increase in feasibility of adsorption at higher temperature. The positive values of $\Delta H°$ indicated that adsorption was endothermic at 20–40 °C. The positive values of $\Delta S°$ confirmed the increased randomness at solid/solution interface during adsorption.

3.5. Fourier transform-infrared spectra (FT-IR) analysis

The functional groups involved in Pb(II) adsorption by MBFGA1 were elucidated using FT-IR spectroscopy. The FT-IR spectra of original and Pb(II)-loaded MBFGA1 in the range of 4000–400 cm^{-1} were taken and presented in Table 4. The FT-IR spectrum of original MBFGA1 showed several distinct and sharp absorption peaks, which indicated the complex nature of the biomass examined. The broad and strong band at 3382 cm^{-1} was due to the overlapping of –OH and –NH$_2$ groups stretching vibration. The absorption peaks at 2933, 1651, 1268, 1130 and 1056 cm^{-1} represented the stretching vibrations of C–H, C=O, C–N, C–O–C and C–O, respectively (Huang et al., 2012). The symmetric and asymmetric bending of –CH$_2$– and –CH$_3$ were observed at 1459 and 1370 cm^{-1}. The latter absorption band at 930 cm^{-1} was assigned to stretching of the glycosidic ring vibration on the biomass surface. In conclusion, the main functional groups on MBFGA1 were carboxyl, amine and hydroxyl, which always played important roles in biosorption of metal cations. According to the spectra of Pb(II)-loaded MBFGA1, the wavenumber and intensity of some absorption peaks were shifted obviously, suggesting the functional groups were in the binding of Pb(II). After Pb(II) adsorption, O–H stretching vibration was shifted to 3368 cm^{-1}. The significant shifts of these specific peaks to the lower wavenumber after the Pb(II) ions were adsorbed suggested that chemical interactions between the Pb(II) ions and the hydroxyl (O–H) groups occurred on the biomass surface. The vanishing of the peaks at 1130 and 930 cm^{-1} might be attributed to the hydrolysis of glycosidic, which could explain the increasing intensity of O–H and C–O. In addition, after loading Pb(II) ions, the peak of –CH$_2$–, –CH$_3$ and C–N groups changed to 1386 cm^{-1}. These

Table 2
Parameters for Langmuir and Freundlich isotherms for Pb(II) adsorption.

Temperature (K)	Langmuir model				Freundlich model		
	q_{max} (mg g^{-1})	K_L (L g^{-1})	R_L	R^2	K_f (mg g^{-1})	n	R^2
293	185.195	3.176	0.0052	0.9943	138.739	4.610	0.8539
303	147.058	8.501	0.0019	0.9906	132.739	5.025	0.9208
313	129.870	9.625	0.0017	0.9963	119.508	4.904	0.9469

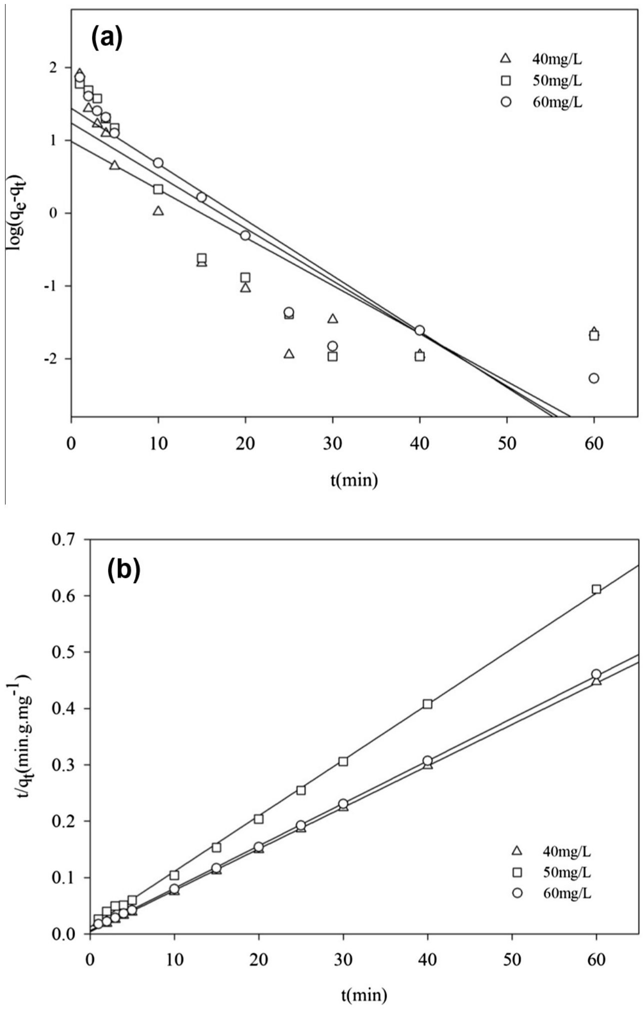

Fig. 3. (a) Pseudo-first-order and (b) pseudo-second-order kinetic model for Pb(II) adsorption onto MBFGA1.

Table 4
Wave number of FT-IR absorption peaks of original MBFGA1 and Pb(II)-loaded MBFGA1.

Activated group	Original MBFGA1	Pb(II)-loaded MBFGA1
–OH and –NH_2	3382	3368
C–H	2933	2971
C=O	1651	1655
–CH_2–	1459	1386
–CH_3	1370	–
C–N	1268	–
C–O–C	1130	–
C–O	1056	1048
Glycosidic ring	930; 883; 815	698

Table 5
EDS analysis of original MBFGA1 and Pb(II)-loaded MBFGA1.

Element	Original MBFGA1			Pb(II)-loaded MBFGA1		
	Energy (keV)	wt%	at%	Energy (keV)	wt%	at%
C	0.3	58.25	69.40	0.3	13.46	40.93
O	0.6	23.39	20.92	0.6	16.33	37.27
S	2.3	0.49	0.22	–	–	–
K	3.2; 3.6	8.74	3.20	–	–	–
Pb	–	–	–	2.3; 10.5; 12.6	60.08	10.59
Ca	–	–	–	3.6	3.25	2.96

results indicated that the functional groups mentioned above were mainly involved in the adsorption of Pb(II) onto MBFGA1 (Sarı et al., 2007). However, the new generated absorption peaks on the spectra of dotted line in the range of 800–400 cm^{-1} demonstrated its strong binding capacity with Pb(II), which might be due to carboxylic groups available for the mechanism of ion exchange.

3.6. Environmental scanning electron microscope (ESEM) analysis

In secondary electron (SE) mode, ESEM micrographs showed that original MBFGA1 prepared by vacuum freeze drying had layered structure and smooth surface morphology. In contrast, Pb(II)-loaded MBFGA1 had compact texture and rough surface morphology. EDS analysis also provided the evidence that the Pb(II) had been bound on the surface of MBFGA1. As is shown in Table 5, the Pb(II) content reached 60.08% in the detection area. These clearly demonstrated a strong coordination linkage between the Pb(II) and the functional groups of MBFGA1. By comparing the typical EDS spectra of original and Pb(II)-loaded MBFGA1, it was observed that the appearance of Pb(II) signal at about 2.3, 10.5 and12.6 keV. The disappearance of S, K signal at about 2.1, 3.2 keV was observed after Pb(II) adsorption. These findings indicated that adsorption process also included ion exchange mechanism for the removal of Pb(II) ions by MBFGA1 (Çabuk et al., 2007).

3.7. Flocculation mechanism

The zeta potential of $Pb(NO_3)_2$ solution was about 40.8 mV at pH 8. After adding 2×10^{-3}% MBFGA1, it turned to be 16.3 mV and then 8.94 mV when 4×10^{-3}% $CaCl_2$ was added. Therefore, charge neutralization may be achieved by addition of Ca^{2+}. The zeta potential of $Pb(NO_3)_2$ solution and removal efficiency during flocculation process were shown in Fig. 4. At the first stage, the removal efficiency firstly increased rapidly and then decreased. But it increased steadily and then reached equilibrium at the second stage. After the first stage, zeta potential appeared to be 8.61 mV. The addition of MBFGA1 aroused a big change in the Zeta potential of $Pb(NO_3)_2$ solution (about −30 mV), which suggested the static repulsive forces among the flocculated particles and indicated that charge neutralization would not be the main Pb(II) removal mechanism at the second stage. The flocculation happened at a high zeta potential of about −23 mV, which meant that adsorption bridging through repulsive obstacle played a major role during the second stage.

Table 3
Pseudo-first-order and pseudo-second-order parameters for the adsorption of Pb(II) onto MBFGA1.

C_0 (mg L^{-1})	Pseudo-first-order			Pseudo-second-order		
	K_1 (min^{-1})	q_e (mg g^{-1})	R^2	k_2 (g mg^{-1} min^{-1})	q_e (mg g^{-1})	R^2
40	0.152	9.596	0.7117	0.014	135.135	0.9996
50	0.167	17.366	0.7554	0.008	101.010	0.9991
60	0.177	27.580	0.8780	0.010	133.333	0.9998

Table 6
Thermodynamic parameters for the adsorption of Pb(II) onto MBFGA1.

Concentration (mg L)	$\Delta H°$ (kJ mol^{-1})	$\Delta S°$ (J mol^{-1} K^{-1})	$\Delta G°$ (kJ mol^{-1})		
			293 K	303 K	313 K
40	11.178	0.078	−11.725	−12.749	−13.294
45	25.850	0.130	−11.990	−14.091	−14.591
50	45.002	0.198	−12.722	−15.256	−16.675
55	21.527	0.113	−11.256	−13.082	−13.509
60	13.288	0.082	−10.290	−12.241	−11.925

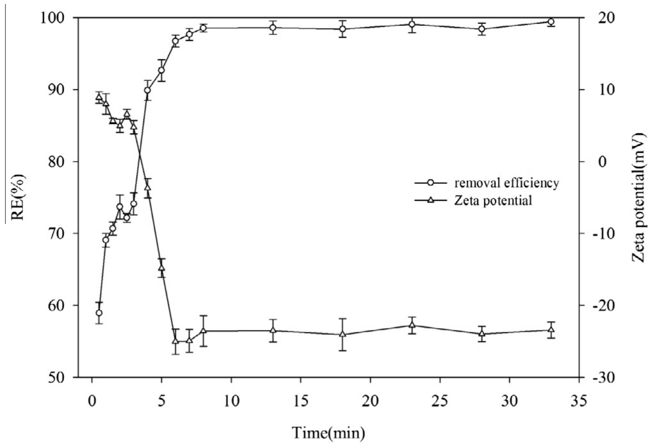

Fig. 4. Zeta potential during the flocculating process.

It could indicate that flocculation of $Pb(NO_3)_2$ solution was completed by charge neutralization and adsorption bridging mechanism in two stages. The main Pb(II) removal mechanism in the first stage was charge neutralization. MBFGA1 had a linear long chain molecular structure mainly composed of rhamnose, xylose, mannose, galactose, glucose, and appeared to have a molecular weight of 1.18×10^6 D (Zhang et al., 2013). It could seize OH^- competitively, making the molecules stretch form a linear structure so that more of the active binding sites emerged. With the increase of pH, OH^- in solution increased. The removal capacity was bigger at higher pH with more OH^- provided. Ca^{2+} reduced the thickness of the diffuse double layer of adjacent colloids, thus reducing the inter particle distance and making MBFGA1 attract more Pb(II) ions around its surface. This phenomenon was well supported by the reduction of zeta potentials close to zero. These interactions were promoted by rapid mixing in jar tests. The pH played an important role in the process. The main Pb(II) removal mechanism in the second stage was adsorption, in which MBFGA1 acted like a bridging agent of many flocs adsorbed Ca^{2+}. Bridging occurred after Ca^{2+} and Pb(II) were adsorbed onto MBFGA1. Moreover, MBFGA1 adsorbed to vacant sites remained on the surface of flocs. Many flocs could be adsorbed onto a long molecular chain. Simultaneously, they could be absorbed by other polymer chains. Thus flocs formed three-dimensional structure with a better settling capacity. Slow mixing allowed the aggregates to combine two or more flocs to form larger floc particles, and precipitate as evidenced in the jar tests (More et al., 2012). The FT-IR, ESEM and desorption analysis illustrated that ion exchange also happened during flocculation process. In desorption experiment, when Pb(II)-loaded MBFGA1 suspended into EDTA (0.5 mol L^{-1}) solution, it dissolved gradually and finally disappeared. It dissolved rapidly with HCl (0.5 mol L^{-1}). There was nothing happened with CH_4N_2O (0.5 mol L^{-1}). The results indicated that ionic bond combination was the main way of combining between MBFGA1 and Pb(II).

4. Conclusions

The present investigation suggested that MBFGA1 is an effective and alternative microbial flocculant for the removal of Pb(II) ions from wastewaters. The maximum removal efficiency was found as 99.85% for Pb(II) ion. The Langmuir isotherm model best fitted the equilibrium data. The adsorption of Pb(II) onto MBFGA1 followed well the pseudo-second-order kinetic model. Based on the results, the main mechanisms of removal Pb(II) by MBFGA1 could be charge neutralization and adsorption bridging. It also indicated the possible application of MBFGA1 to solve the serious problems caused by heavy metal ions pollution.

Acknowledgement

This study was supported by National Natural Science Foundation of China (30970105 and 51078131).

References

Aydın, Y.A., Aksoy, N.D., 2009. Adsorption of chromium on chitosan: Optimization, kinetics and thermodynamics. Chemical Engineering Journal 151, 188–194.

Çabuk, A., Akar, T., Tunali, S., Gedikli, S., 2007. Biosorption of Pb(II) by industrial strain of *Saccharomyces cerevisiae* immobilized on the biomatrix of cone biomass of *Pinus nigra*: Equilibrium and mechanism analysis. Chemical Engineering Journal 131, 293–300.

Chakravarty, S., Mohanty, A., Sudha, T.N., Upadhyay, A.K., Konar, J., Sircar, J.K., Madhukar, A., Gupta, K.K., 2010. Removal of Pb(II) ions from aqueous solution by adsorption using bael leaves (*Aegle marmelos*). Journal of Hazardous Materials 173, 502–509.

Chen, W., Wu, C., James, E., Chang, J., 2008. Metal biosorption capability of *Cupriavidus taiwanensis* and its effects on heavy metal removal by nodulated *Mimosa pudica*. Journal of Hazardous Materials 151, 364–371.

Fu, F.L., Wang, Q., 2011. Removal of heavy metal ions from wastewaters: a review. Journal of Environmental Management 92, 407–418.

Gao, Q., Zhu, X.H., Mu, J., Zhang, Y., Dong, X.W., 2009. Using *Ruditapes philippinarum* conglutination mud to produce bioflocculant and its applications in wastewater treatment. Bioresource Technology 100, 4996–5001.

Gao, W.C., Yang, Z.H., Huang, J., Deng, J.H., Xu, H.Y., Xie, H.M., 2011. Optimization of response surface and the mechanism study of microbial flocculants on capturing Cu(II). Chinese Journal of Environmental Engineering 5, 2411–2416.

Ghorai, S., Sinhamahpatra, A., Sarkar, A., Panda, A.B., Pal, S., 2012. Novel biodegradable nanocomposite based on XG-g-PAM/SiO_2: application of an efficient adsorbent for Pb^{2+} ions from aqueous solution. Bioresource Technology 119, 181–190.

Hu, X.J., Wang, J.S., Liu, Y.G., Li, X., Zeng, G.M., Bao, Z.L., Zeng, X.X., Chen, A.W., Long, F., 2011. Adsorption of chromium(VI) by ethylenediamine-modified cross-linked magnetic chitosan resin: isotherms, kinetics and thermodynamics. Journal of Hazardous Materials 185, 306–314.

Huang, J., Yang, Z.H., Zeng, G.M., Ruan, M., Xu, H.Y., Gao, W.C., Luo, Y.L., Xie, H.M., 2012. Influence of composite flocculant of PAC and MBFGA1 on residual aluminum species distribution. Chemical Engineering Journal 191, 269–277.

Karatas, M., 2012. Removal of Pb(II) from water by natural zeolitic tuff: kinetics and thermodynamics. Journal of Hazardous Materials 199–200, 383–389.

Karthikeyan, S., Balasubramanian, R., Iyer, C.S.P., 2007. Evaluation of the marine algae *Ulva fasciata* and *Sargassum* sp. for the biosorption of Cu(II) from aqueous solutions. Bioresource Technology 98, 452–455.

Kogej, A., Pavko, A., 2001. Comparison of *Rhizopus nigricans* in a pelleted growth form with some other types of waste microbial biomass as biosorbents for metal ions. World Journal of Microbiology & Biotechnology 17, 677–685.

Lee, B.J., Schlautman, M.A., Toorman, E., Fettweis, M., 2012. Competition between kaolinite flocculation and stabilization in divalent cation solutions dosed with anionic polyacrylamides. Water Research 46, 5696–5706.

Li, W.W., Zhou, W.Z., Zhang, Y.Z., Wang, J., Zhu, X.B., 2008. Flocculation behavior and mechanism of an exopolysaccharide from the deep-sea psychrophilic bacterium *Pseudoalteromonas* sp. SM9913. Bioresource Technology 99, 6893–6899.

Lian, B., Chen, Y., Zhao, J., Teng, H.H., Zhu, L., Yuan, S., 2008. Microbial flocculation by *Bacillus mucilaginosus*: applications and mechanisms. Bioresource Technology 99, 4825–4831.

Matheickal, J., Yu, Q., 1999. Biosorption of lead(II) and copper(II) from aqueous solutions by pre-treated biomass of Australian marine algae. Bioresource Technology 69, 223–229.

Moon, S.-H., Park, C.-S., Kim, Y.-J., Park, Y.-I., 2006. Biosorption isotherms of Pb(II) and Zn(II) on Pestan, an extracellular polysaccharide, of *Pestalotiopsis* sp. KCTC 8637P. Process Biochemistry 41, 312–316.

More, T.T., Yan, S., Hoang, N.V., Tyagi, R.D., Surampalli, R.Y., 2012. Bacterial polymer production using pre-treated sludge as raw material and its flocculation and dewatering potential. Bioresource Technology 121, 425–431.

Prasertsan, P., Dermlim, W., Doelle, H., Kennedy, J.F., 2006. Screening, characterization and flocculating property of carbohydrate polymer from newly isolated *Enterobacter cloacae* WD7. Carbohydrate Polymers 66, 289–297.

Salehizadeh, H., Shojaosadati, S.A., 2001. Extracellular biopolymeric flocculants. Recent trends and biotechnological importance. Biotechnology Advances 19, 371–385.

Sarı, A., Tuzen, M., Uluözlü, Ö.D., Soylak, M., 2007. Biosorption of Pb(II) and Ni(II) from aqueous solution by lichen (*Cladonia furcata*) biomass. Biochemical Engineering Journal 37, 151–158.

Schneegurt, M.A., Jain, J.C., Menicucci, J.A., Brown, S.A., Kemner, K.M., Garofalo, D.F., Quallick, M.R., Neal, C.R., Kulpa, C.F., 2001. Biomass byproducts for the remediation of wastewaters contaminated with toxic metals. Environmental Science & Technology 35, 3786–3791.

Senthilkumar, R., Vijayaraghavan, K., Thilakavathi, M., Iyer, P.V.R., Velan, M., 2007. Application of seaweeds for the removal of lead from aqueous solution. Biochemical Engineering Journal 33, 211–216.

Shih, I.L., Van, Y.T., Yeh, L.C., Lin, H.G., Chang, Y.N., 2001. Production of a biopolymer flocculant from *Bacillus licheniformis* and its flocculation properties. Bioresource Technology 78, 267–272.

Sobeck, D.C., Higgins, M.J., 2002. Examination of three theories for mechanisms of cation-induced bioflocculation. Water Research 36, 527–538.

Velmurugan, N., Hwang, G., Sathishkumar, M., Choi, T.K., Lee, K.-J., Oh, B.-T., Lee, Y.-S., 2010. Isolation, identification, Pb(II) biosorption isotherms and kinetics of a lead adsorbing *Penicillium* sp. MRF-1 from South Korean mine soil. Journal of Environmental Sciences 22, 1049–1056.

Xu, D., Tan, X.L., Chen, C.L., Wang, X.K., 2008. Adsorption of Pb(II) from aqueous solution to MX-80 bentonite: effect of pH, ionic strength, foreign ions and temperature. Applied Clay Science 41, 37–46.

Yan, G., Viraraghavan, T., 2003. Heavy-metal removal from aqueous solution by fungus *Mucor rouxii*. Water Research 37, 4486–4496.

Yang, Z., Tao, R., Zeng, G., Xiao, Y., Deng, E., 2006. Culture medium and grading culture techniques for bioflocculant production by *Paenibacillus polymyxa* GA1. Environmental Science 27, 1444–1449 (in Chinese).

Yang, Z.-H., Huang, J., Zeng, G.-M., Ruan, M., Zhou, C.-S., Li, L., Rong, Z.-G., 2009. Optimization of flocculation conditions for kaolin suspension using the composite flocculant of MBFGA1 and PAC by response surface methodology. Bioresource Technology 100, 4233–4239.

Zhang, Z.Q., Lin, B., Xia, S.Q., Wang, X.J., Yang, A.M., 2007. Production and application of a novel bioflocculant by multiple-microorganism consortia using brewery wastewater as carbon source. Journal of Environmental Sciences 19, 667–673 (in Chinese).

Zhang, Y.Y., Yang, Z.H., Zeng, G.M., Huang, J., Wei, S.M., Feng, J., 2013. Microbial flocculant MBFGA1 preliminary structure identification and research on flocculation mechanism. Environmental Science 33, 278–285 (in Chinese).